

Interdecadal change in the relationship of southern China summer rainfall with tropical Indo-Pacific SST

Renguang Wu · Song Yang · Zhiping Wen ·
Gang Huang · Kaiming Hu

Received: 29 March 2011 / Accepted: 26 August 2011 / Published online: 10 September 2011
© Springer-Verlag 2011

Abstract The present study investigates the interdecadal change in the relationship between southern China (SC) summer rainfall and tropical Indo-Pacific sea surface temperature (SST). It is found that the pattern of tropical Indo-Pacific SST anomalies associated with SC summer rainfall variability tends to be opposite between the 1950–1960s and the 1980–1990s. Above-normal SC rainfall corresponds to warmer SST in the tropical southeastern Indian Ocean (SEIO) and cooler SST in the equatorial central Pacific (ECP) during the 1950–1960s but opposite SST anomalies in these regions during the 1980–1990s. A pronounced difference is also found in anomalous atmospheric circulation linking SEIO SST and SC rainfall

between the two periods. In the 1950–1960s, two anomalous vertical circulations are present between ascent over SEIO and ascent over SC, with a common branch of descent over the South China Sea that is accompanied by an anomalous low-level anticyclone. In the 1980–1990s, however, a single anomalous vertical circulation directly connects ascent over SC to descent over SEIO. The change in the rainfall–SST relationship is likely related to a change in the magnitude of SEIO SST forcing and a change in the atmospheric response to the SST forcing due to different mean states. A larger SEIO SST forcing coupled with a stronger and more extensive western North Pacific subtropical high in recent decades induce circulation anomalies reaching higher latitudes, influencing SC directly. Present analysis shows that the SEIO and ECP SST anomalies can contribute to SC summer rainfall variability both independently and in concert. In comparison, there are more cases of concerted contributions due to the co-variability between the Indian and Pacific Ocean SSTs.

R. Wu
Institute of Space and Earth Information Science and Department
of Physics, The Chinese University of Hong Kong,
Shatin, New Territories, Hong Kong

S. Yang
Climate Prediction Center, NOAA,
Camp Springs, MD, USA

Z. Wen
Center for Monsoon and Environment Research,
Sun Yat-Sen University,
Guangzhou, China

G. Huang · K. Hu
Institute of Atmospheric Physics, Chinese Academy of Sciences,
Beijing, China

R. Wu (✉)
Institute of Space and Earth Information Science,
Fok Ying Tung Remote Sensing Science Building,
The Chinese University of Hong Kong,
Shatin, NT,
Hong Kong, China
e-mail: renguang@cuhk.edu.hk

1 Introduction

Summer flooding and drought occur frequently in China and cause significant economic loss. Understanding the factors and physical processes for summer rainfall anomalies is of great socio-economic importance for China's sustainable development. Thus, the variability of summer rainfall and its causes have been a topic of many previous studies. Anomalous summer rainfall in China has been attributed to the influences of sea surface temperature (SST) in the tropical Indo-Pacific Oceans (e.g., Huang and Sun 1992; Weng et al. 1999; Zhang et al. 1996, 1999; Lau and Weng 2001; Xiao et al. 2002; Huang et al. 2003; Wu et al. 2003; Yang and Lau 2006) and land surface state in the

Eurasian continent such as snow cover (Yang and Xu 1994; Chen and Wu 2000; Wu and Qian 2003; Wu and Kirtman 2007; Zhao et al. 2007) and soil moisture (Yang and Lau 1998).

One important factor for summer rainfall variability in China is El Niño-Southern Oscillation (ENSO). Summer rainfall tends to be above normal in the Yangtze-Huaihe River region and below normal in South and North China during the El Niño decaying years (Huang and Wu 1989). It was also found that ENSO has a weak correlation with summer rainfall in southern China (SC) for the period 1950–2000 (Wu et al. 2003), which is consistent with the small summer rainfall difference in SC between the El Niño and La Niña events (Lau and Weng 2001).

Further analysis, however, indicates that the correlation of SC summer rainfall with the tropical Indo-Pacific SST has experienced an obvious interdecadal change around the mid-1970s. Figure 1 shows the correlation of SC summer (June–August (JJA)) rainfall with contemporaneous SST in the tropical Indo-Pacific domain. The SC rainfall is defined as the average of rainfall at 33 stations located to the east of 105° E and to the south of 28.5° N. For the whole period (1951–2006), no obvious correlation can be observed (Fig. 1a). When the correlation is calculated for 21-year sub-periods, however, significant correlation appears. For 1951–1971, positive correlation is seen in the regions around the Maritime Continent, and negative correlation is found in the equatorial central and eastern Pacific (Fig. 1b). For 1978–1998, negative correlation is seen in the southeastern Indian Ocean (SEIO) and the Maritime Continent, and positive correlation is observed in the equatorial central Pacific (ECP) (Fig. 1c). Apparently, the correlation in the tropical Indo-Pacific region is very different between the two sub-periods, displaying a tendency of opposite signs in many regions. The selection of the above two sub-periods will be justified later.

The main purpose of the present study is to investigate and understand the above interdecadal change. The organization of this paper is as follows. The datasets used in the present study are described in Section 2. Section 3 presents evidence for the interdecadal change in the relationship of SC summer rainfall with SST and atmospheric circulation. Section 4 addresses the influence of SEIO and ECP SST anomalies using conditional composite. Section 5 discusses the plausible reasons for the interdecadal change in the rainfall–SST relationship. A summary of the results obtained is given in Section 6.

2 Datasets

The present study uses monthly mean rainfall of 160 stations in China from 1951 to 2008, which is provided by

the National Climate Center of the China Meteorological Administration. The following two precipitation datasets are used for validation. One is the monthly mean precipitation reconstruction data over land produced by the National Oceanic and Atmospheric Administration (NOAA) Climate Prediction Center (CPC) (Chen et al. 2002), which is available on 0.5°×0.5° grid since January 1948. The other is the monthly mean CPC Merged Analysis of Precipitation (Xie and Arkin 1997), which is available on 2.5°×2.5° grid starting from January 1979.

This study also uses the NOAA Extended Reconstruction SST, version 3 (Smith et al. 2008), which is provided by NOAA/OAR/ESRL Physical Science Division, Boulder, Colorado, USA and obtained from its website at <http://www.cdc.noaa.gov/>. This SST dataset has a resolution of 2.0°×2.0° and is available from 1854 to present. The winds at 200 and 850 hPa and vertical velocity at 500 hPa from the National Centers for Environmental Prediction–National Center for Atmospheric Research (NCEP–NCAR) reanalysis product (Kalnay et al. 1996) are analyzed in this study. The velocity potential derived from winds is also analyzed. These variables are available on 2.5°×2.5° grids from 1948 to present.

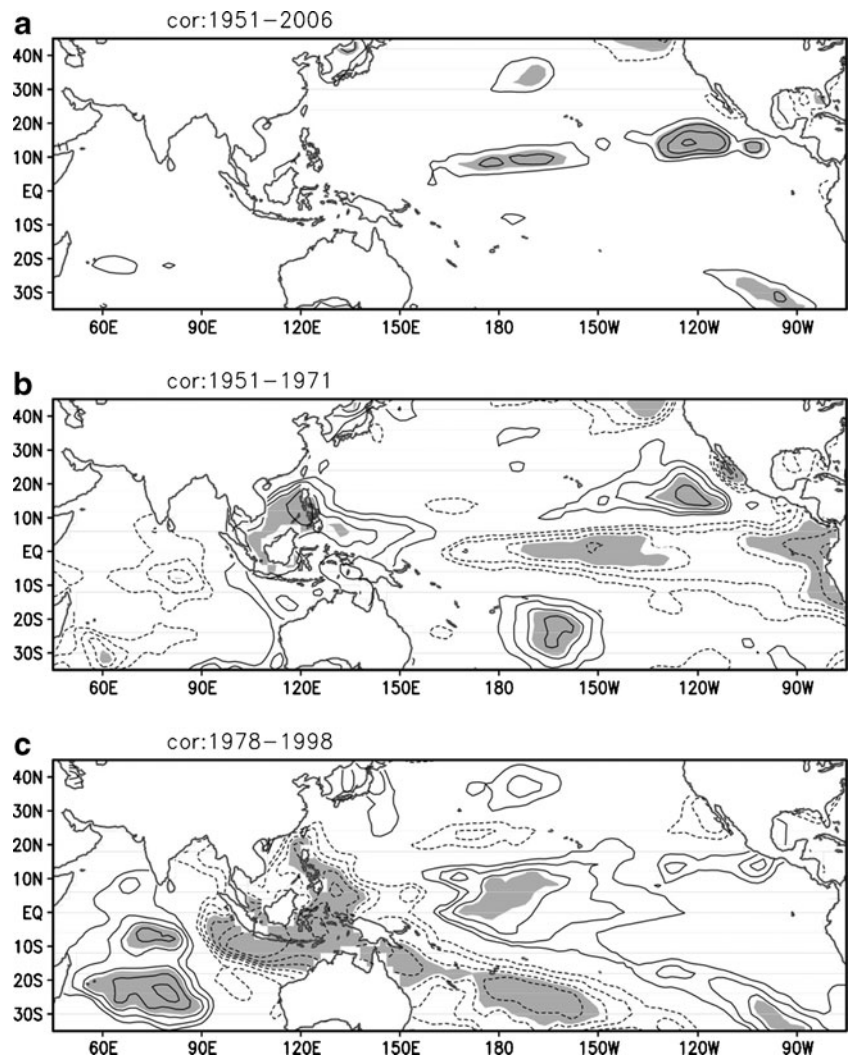
Throughout this study, the analysis is performed for interannual variations on time scales shorter than 8 years. Variations of 8 years and longer time scales have been removed using a harmonic analysis. This approach is applied to exclude the plausible contamination of interannual relationship by interdecadal changes and to avoid the impact of plausible unrealistic interdecadal variability in the NCEP–NCAR reanalysis (Yang et al. 2002; Inoue and Matsumoto 2004; Wu et al. 2005).

3 Interdecadal change in the interannual rainfall–SST relationship

In this section, we start with a further contrast of the correlation of SC summer rainfall with SST before and after the mid-1970s. This is followed by a comparison of the evolution of corresponding SST anomalies. The associated atmospheric circulation anomalies are then examined to understand the processes connecting SC summer rainfall to the SST forcing.

As is shown in Fig. 1, the correlation of SST with SC summer rainfall changes from positive to negative in SEIO, whereas it changes from negative to positive in ECP around the mid-1970s. This change is further illustrated in Fig. 2 that shows the 21-year sliding correlation of SST anomalies in the NINO4 region (5° S–5° N, 160° E–150° W) and the SEIO region (20–5° S, 100–130° E) with SC JJA rainfall anomalies. The sliding correlation before mid-1960s is positive for SEIO SST but negative for NINO4 SST. After

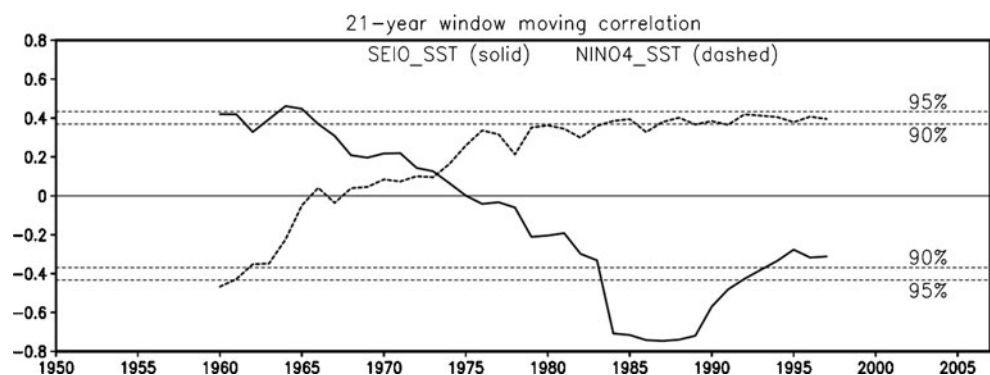
Fig. 1 Correlation coefficient of JJA SST with JJA SC rainfall for 1951–2006 (a), 1951–1971 (b), and 1978–1998 (c). Contour interval is 0.2 and the contours with the magnitude less than 0.2 are suppressed. Shading denotes correlation coefficient larger than 0.433, which is significant at the 95% confidence level



the mid-1970s, the sliding correlation is negative for SEIO SST, but positive for NINO4 SST. Years 1961 and 1978 are approximately the center years when the two 21-year sliding correlations are most significant and opposite. Thus, we choose 1951–1971 and 1978–1998 as the two sub-periods in the following correlation and regression analyses to understand the different relationship between SC summer rainfall and tropical Indo-

Pacific SSTs. The correlation coefficients in 1951–1971 are +0.42 for SEIO SST and -0.43 for NINO4 SST, respectively. The correlation coefficients in 1978–1998 are -0.74 for SEIO SST and +0.40 for NINO4 SST, respectively. The differences of above correlation coefficients between 1951 and 1971 and 1978 and 1998 are significant at the 95% confidence level according to a test based on the Fisher's Z-transform.

Fig. 2 Moving correlation coefficient of SEIO (solid curve) and NINO4 JJA SST (dashed curve) with SC JJA rainfall with a 21-year window. The correlation is shown at the center year of the 21-year window



The change in the correlation is also reflected in the change in the relative frequency of opposite-sign and same-sign relationships between SST and rainfall anomalies. We use the 0.5 standard deviations as a criterion to determine an anomalous year of rainfall or SST. The rainfall and SST anomalies show both same-sign and opposite-sign relationships. The numbers of same-sign and opposite-sign cases are shown in Table 1 for 1951–1974 and 1975–2007. The selection of the two periods is based on the sliding correlation. For SEIO SST, there are much more same-sign years (nine) than opposite-sign years (one) during 1951–1974, whereas there are more opposite-sign years (14) than same-sign years (six) during 1975–2007. On the contrary, for NINO4 SST, there are more opposite-sign years (eight) than same-sign years (four) during 1951–1974, whereas same-sign years (12) overwhelm opposite-sign years (one) during 1975–2007.

For a better understanding of the relationship, we show in Fig. 3 the SST anomalies in different seasons obtained by regression onto normalized SC summer rainfall anomalies for the two sub-periods separately. In the figure, the notations for seasons follow the tradition, i.e., December–January–February (DJF), March–April–May (MAM), June–July–August (JJA), and September–October–November (SON). The seasons in the same year as SC summer rainfall are denoted with “(0)” and those in the succeeding year are denoted with “(1).”

The SST anomalies in the equatorial Pacific display different spatial-temporal evolution. Negative SST anomalies move westward from spring to winter during 1951–1971 (Fig. 3a), whereas positive SST anomalies displace eastward during 1978–1998 (Fig. 3b). Similar feature is seen in the correlation of SST with early summer (May–June) southeast China rainfall (Chang et al. 2000). Thus, above-normal SC summer rainfall is observed in the developing years of La Niña events for the former period, but in the developing years of El Niño events for the latter period, which is consistent with Zhu et al. (2007).

Very different SST anomalies are also seen in the tropical Indian Ocean. During 1951–1971, positive SST anomalies dominate in the preceding winter (DJF (0)). The SST anomalies are weak in MAM (0). Weak negative SST

anomalies appear in JJA (0) and SON (0) except for SEIO. In the following winter (DJF (1)), negative SST anomalies dominates. During 1978–1998, negative SST anomalies are seen in equatorial and South Indian Ocean in the preceding winter. During MAM (0) through SON (0), negative SST anomalies increase in SEIO. In JJA (0) and SON (0), positive SST anomalies develop in central and western tropical Indian Ocean.

In SEIO, positive SST anomalies are seen in JJA (0) and SON (0) during 1951–1971 (Fig. 3a) but negative SST anomalies are noticed during 1978–1998 (Fig. 3b). In SON (0), negative and positive Indian Ocean Dipole (IOD; Saji et al. 1999) patterns are observed in the former and latter periods, respectively. The distribution of SST anomalies in the tropical Indian Ocean suggests a link between SC summer rainfall and summer IOD. Weng et al. (2009) identified a positive correlation between summer IOD and SC summer rainfall for 1951–2007. The present analysis indicated that the positive correlation is mainly contributed by the period after the late-1970s. Indeed, the amplitude of the IOD is larger after the mid-1970s (e.g., Annamalai et al. 2005) and thus may dominate the correlation for the period 1951–2007. Ding et al. (2010) obtained an IOD pattern in the correlation of summer SST anomalies with an East Asian summer monsoon index (Li and Zeng 2002) during 1953–1975, but not during 1978–2000. Furthermore, from Fig. 3, the correlation in the western pole of the IOD is weak in JJA (0). Thus, the correlation with summer IOD comes mainly from the eastern pole of the IOD.

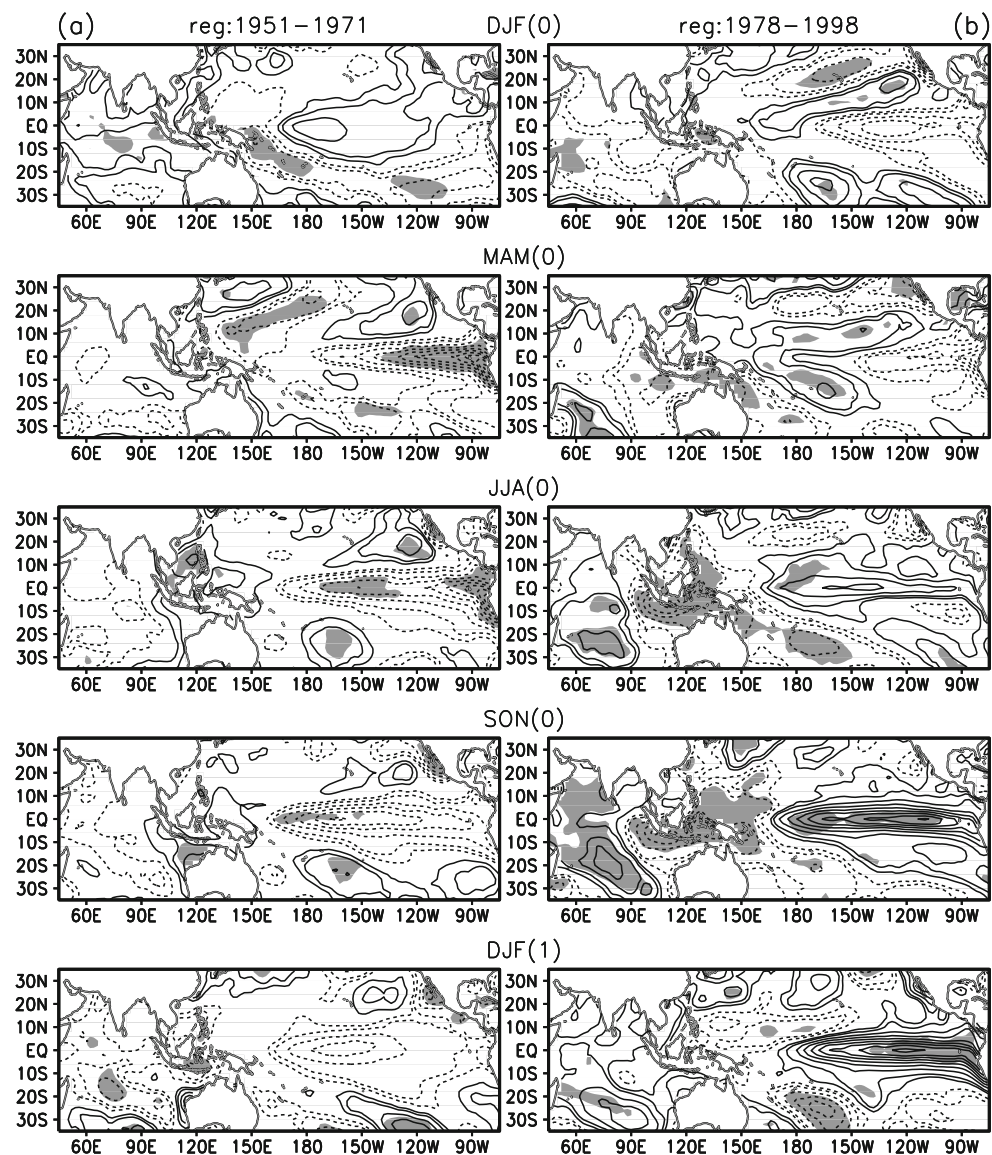
In the South China Sea (SCS) and western North Pacific (WNP) region, SST anomalies display a switch from negative to positive from MAM (0) to JJA (0) and positive anomalies decay after JJA (0) during 1951–1971 (Fig. 3a). The SST anomalies during 1978–1998 show a similar change except for opposite signs. Note that the negative SST anomalies in the WNP are most significant after JJA (0). For both periods, the SST anomalies are opposite between the SEIO and NINO4 regions. This feature is related to the relationship between the Pacific and Indian Ocean SST variations. El Niño is often accompanied by negative SST anomalies in SEIO, as discussed in previous studies (e.g., Huang and Kinter 2002; Xie et al. 2002; Wu et al. 2008; Wu and Yeh 2010).

To understand the connection of SC rainfall to Indo-Pacific SST and its change, we show in Fig. 4 anomalies of winds at 850 and 200 hPa and vertical velocity at 500 hPa obtained by regression on normalized JJA SC rainfall. During 1951–1971, 850 hPa winds show cross-equatorial northerlies over the Maritime Continent, an anomalous anticyclone over SCS and WNP, and an anomalous cyclone over SC (Fig. 4a). Over the mid-latitudes of East Asia is an anomalous anticyclone. Thus, the wind anomalies feature a meridional wave pattern over WNP and East Asia. At

Table 1 Number of cases when JJA SEIO or NINO4 SST anomalies have the sign same as or opposite to SC JJA rainfall anomalies during 1951–1974 and 1975–2007

	SEIO SST		NINO4 SST	
	1951–1974	1975–2007	1951–1974	1975–2007
Same sign	9	6	4	13
Opposite sign	1	14	8	1

Fig. 3 SST anomalies in DJF (0), MAM (0), JJA (0), SON (0), and DJF (1) obtained by regression on normalized JJA (0) SC rainfall for 1951–1971 (a) and 1978–1998 (b). Contour interval is 0.08°C (0.04°C) for magnitudes larger (less) than 0.08°C (0.04°C) with zero contours suppressed. Shading denotes the corresponding correlation coefficient larger than 0.433, which is significant at the 95% confidence level

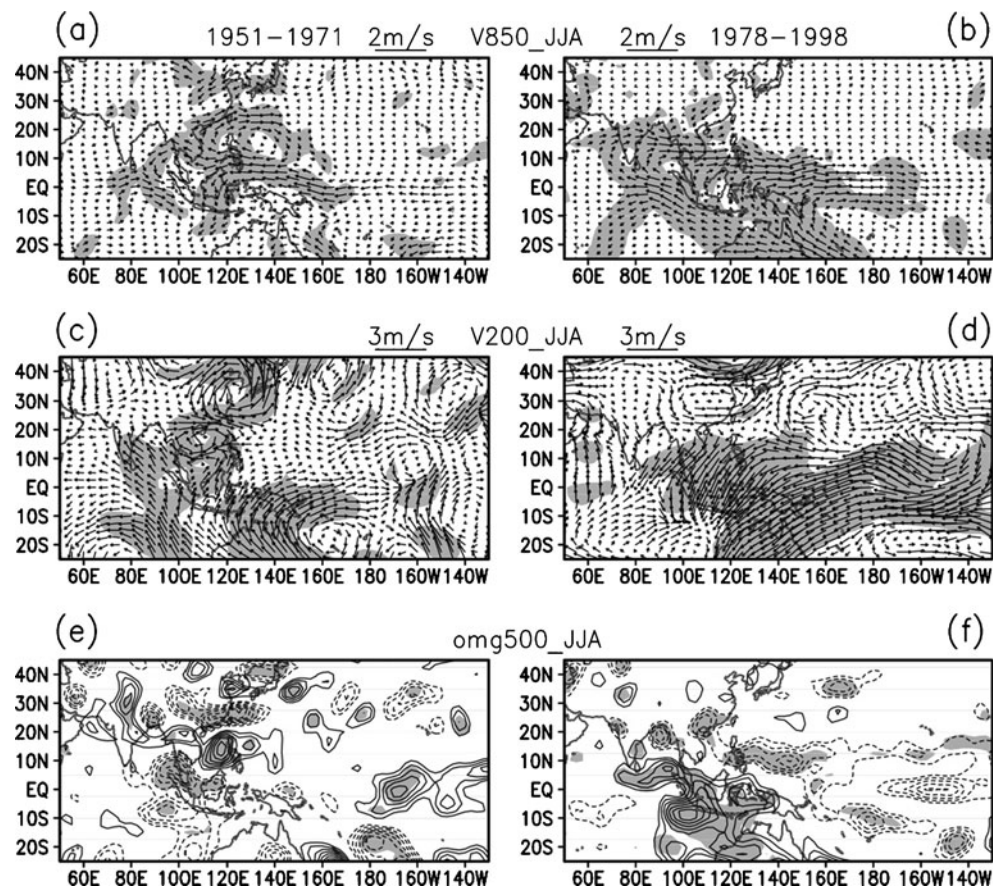


200 hPa, there are cross-equatorial southerlies from the Southern Hemisphere to the Bay of Bengal and SCS, leading to convergence extending over northern Indian through the Indochina Peninsula and SCS to WNP (Fig. 4c). A meridional wave pattern is visible from SCS to East Asia. The 500 hPa vertical motion displays anomalous ascent over SEIO, the Maritime Continent, and the Malay Peninsula (Fig. 4e). It also displays anomalous descent over SCS and WNP, and anomalous ascent over SC. The distribution features a tripole pattern over the Maritime Continent, SCS, and SC. The tripole pattern is confirmed by the correlation of precipitation derived from Chen et al. (2002) that is positive over the Maritime Continent, negative over the Philippine Islands and northern Indochina Peninsula, and positive over SC (not shown). The lower-level convergence, upper-level divergence, and mid-tropospheric ascent suggest the role of positive SST

anomalies in SEIO. According to Lindzen and Nigam (1987), warm SST anomalies reduce surface pressure, inducing lower-level convergence and upward motion. Over the equatorial western Pacific are low-level easterlies (Fig. 4a) and upper-level westerlies (Fig. 4c). Anomalous descent is seen over ECP (Fig. 4e). These circulation anomalies feature a response to negative SST anomalies in ECP (Fig. 3a).

During 1978–1998, at 850 hPa, strong anticyclonic winds cover the regions from northern Australia to the Maritime Continent and the Bay of Bengal, and anomalous cyclonic winds dominate the WNP, northern SCS, and SC regions (Fig. 4b). At 200 hPa, northeasterly anomalies blow from the WNP and ECP regions to SEIO and northern Australia (Fig. 4d). The 500 hPa vertical motion anomalies show descent over SEIO, the Maritime Continent, and the equatorial eastern Indian Ocean, and ascent over the ECP,

Fig. 4 Anomalies of 850 hPa winds (a, b), 200 hPa winds (c, d), and 500 hPa p -vertical velocity (e, f) obtained by regression on normalized JJA SC rainfall for 1951–1971 (left) and 1978–1998 (right). The wind scale is shown at the top of the respective panels. The contour interval for 500-hPa p -vertical velocity is 0.001 Pa s^{-1} , and the contours with the magnitude less than 0.002 Pa s^{-1} are suppressed. Shading denotes the corresponding correlation vector or coefficient larger than 0.433, which is significant at the 95% confidence level



the WNP, the Bay of Bengal, and SC (Fig. 4f). These descent and ascent anomalies form a northeast-southwest dipole pattern, which is confirmed by the correlation of precipitation of Chen et al. (2002) and Xie and Arkin (1997) (figures not shown) that is negative over the Maritime Continent and positive over SC and the Philippine Islands. The circulation anomalies appear to be responses to both negative SST anomalies in SEIO and positive SST anomalies in ECP. These SST anomalies form an east-west contrast. Together, they induce anomalous heating over the ECP and anomalous cooling over the Maritime Continent. In response, lower-level westerlies and upper-level easterlies develop over the equatorial western Pacific. These are accompanied by upper-level convergence over SEIO. The lower-level anticyclone extending from northern Australia to the Bay of Bengal features a Rossby wave type response to anomalous cooling over SEIO.

The upper-level and lower-level anomalous winds suggest a close connection between the atmospheric circulation over SC and WNP and that over the SEIO. To provide further evidence for the connection, we analyze anomalies of velocity potential at 200 and 850 hPa obtained by regression on normalized JJA SC rainfall. During 1951–1971, at 200 hPa, there is anomalous divergence over northern Australia and SEIO, anomalous convergence over

the SCS, WNP, and ECP, and anomalous divergence over SC (Fig. 5a). The divergent winds flow from northern Australia and SEIO to the SCS and WNP, where they converge with those from SC. At 850 hPa, opposite anomalies of divergence and convergence are seen in the above regions (Fig. 5c). The divergent winds are also opposite to those at 200 hPa. During 1978–1998, at 200 hPa, there is anomalous convergence over SEIO, anomalous divergence over WNP and the equatorial western Pacific, with northerlies blowing from SC to SEIO (Fig. 5b). At 850 hPa, anomalous divergence is seen over SEIO, and anomalous convergence over WNP and SC, with southerlies blowing from the Maritime Continent to SC (Fig. 5d).

The above features indicate an anomalous cross-equatorial vertical circulation between SEIO and northern SCS, and another anomalous vertical cell between northern SCS and SC during 1951–1971. This is demonstrated by Fig. 6a that shows the latitude-altitude cross section of anomalous vertical motion and meridional divergence wind averaged over $105\text{--}120^\circ \text{ E}$ for 1951–1971. Clearly, there are two vertical cells between SEIO and SC with a common branch over the SCS. During 1978–1998, an anomalous vertical circulation connects directly the descent over SEIO and the Maritime Continent to the ascent over SC. This is

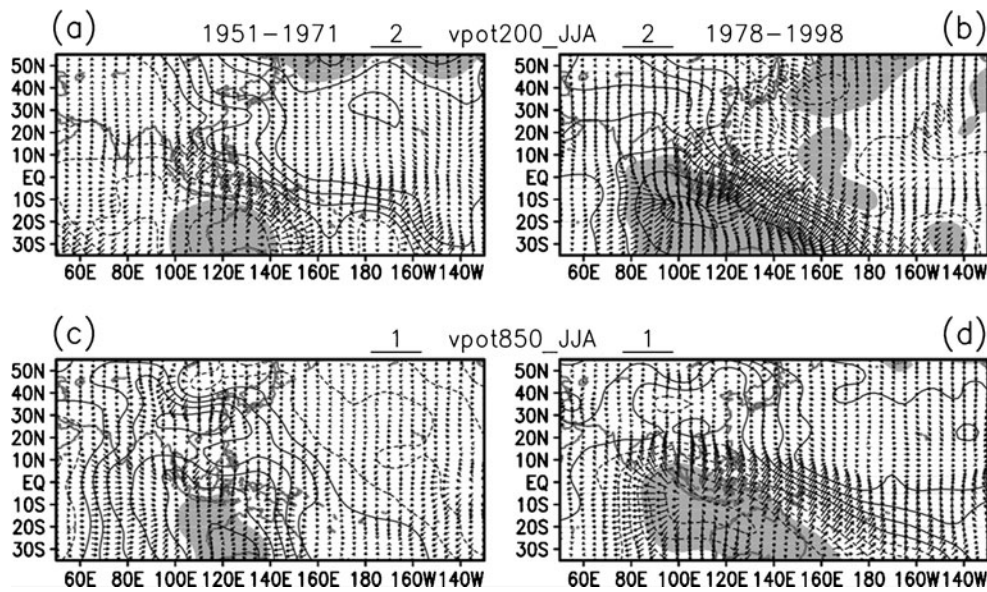


Fig. 5 Anomalies of velocity potential at 200 (a, b) and 850 hPa (c, d) and the corresponding divergent winds obtained by regression on normalized JJA SC rainfall for 1951–1971 (left) and 1978–1998 (right). The wind scale is shown at the top of the respective panels.

The contour interval is $0.1 \times 10^6 \text{ s}^{-1}$. Shading denotes the corresponding correlation coefficient larger than 0.433, which is significant at the 95% confidence level

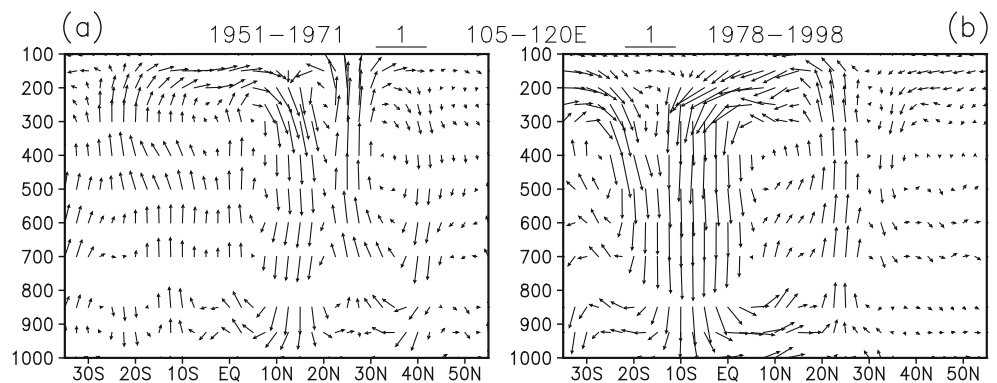
confirmed by Fig. 6b, which is similar to Fig. 6a except for 1978–1998.

Given the significant SST anomalies in the SEIO, the above feature suggests that the SEIO SST forcing may play an important role in the SC summer rainfall variability through anomalous vertical circulation. However, the SEIO SST-SC rainfall relationship is opposite between 1951 and 1971 and 1978 and 1998 because of the pronounced difference in the anomalous vertical circulation between SEIO and SC. During 1951–1971, there are two vertical cells between SEIO and SC and as such positive (negative) SEIO SST anomalies are accompanied by above-normal (below-normal) SC rainfall, leading to a positive SEIO SST-SC rainfall correlation. In contrast, during 1978–1998, only a single vertical cell is present between SEIO and SC and thus positive (negative) SEIO SST anomalies are accompanied by below-normal (above-normal) SC rainfall,

leading to a negative SEIO SST-SC rainfall correlation. A question is why the anomalous circulation associated with SC summer rainfall is so different between the two periods. This will be discussed in Section 5.

The anomalous circulation over the tropical western-central Pacific features a response to SST anomalies in ECP. Corresponding to negative SST anomalies in ECP are anomalous descent over ECP and lower-level easterlies and upper-level westerlies over the equatorial western Pacific. The tropical circulation over the Maritime Continent and the equatorial western-central Pacific suggests a close east-west connection, a feature often seen during ENSO (e.g., Wang et al. 2003). Thus, the SEIO and ECP SST anomalies appear to act in concert and the observed feature is likely a result of the combined effects of both SEIO and ECP SSTs. One question is what the respective influence of SEIO and ECP SST anomalies is.

Fig. 6 Composite anomalies of vertical circulation consisting of divergent meridional wind (m/s) and vertical p -velocity (0.01 Pa/s) along $105\text{--}120^\circ\text{E}$ obtained by regression on normalized JJA SC rainfall for 1951–1971 (a) and 1978–1998 (b). The vertical p -velocity has been multiplied by -100 for displaying purpose. The vector scale is shown at the top of the respective panels



4 Composite analysis for the influence of SST anomalies

Previous section suggests that both the SEIO and ECP SST anomalies may contribute to SC summer rainfall variability through changes in atmospheric circulation. The regression or correlation analysis in the previous section, however, cannot determine whether the circulation anomalies are due to the impacts of SEIO or SCP SST anomalies or both. In this section, we perform a conditional composite analysis to understand the combined and individual influences of SEIO and ECP SST anomalies on atmospheric circulation and SC rainfall.

As is shown in Table 1, SEIO SST and SC rainfall anomalies are dominated by the same-sign relationship during 1951–1974, whereas they display more years of opposite-sign relationship than same-sign relationship during 1975–2007. NINO4 SST and SC rainfall anomalies show more years of same-sign relationship than opposite-sign relationship during 1951–1974 but are dominated by the same-sign relationship during 1975–2007. The specific years for these types of cases are listed in Table 2. From the table, during 1951–1974, there are 4 years (1951, 1955, 1964, and 1965) in which same-sign SEIO SST-SC rainfall relationship is coupled with opposite-sign NINO4 SST-SC rainfall relationship. During 1975–2007, there are 10 years (1975, 1978, 1982, 1984, 1986, 1989, 1996, 1997, 1998, and 2006) in which opposite-sign SEIO SST-SC rainfall relationship is coupled with same-sign NINO4 SST-SC rainfall relationship. In all these years, SEIO and ECP SST anomalies may contribute constructively to the observed rainfall anomalies. During 1951–1974, there are 4 years (1953, 1954, 1957, and 1963) in which SEIO SST is near normal and NINO3 SST anomalies are opposite to SC rainfall anomalies. In these cases, ECP SST anomalies contribute independently to SC rainfall anomalies. During 1975–2007, there are 4 years (1976, 1979, 1992, and 1994) in which SEIO SST anomalies are opposite to SC rainfall anomalies and NINO4 SST is near normal. In these cases,

SEIO SST anomalies contribute independently to SC rainfall anomalies.

We construct composite anomalies for the above four types of cases. In constructing the composite, we multiply the anomalies by -1 when SC summer rainfall anomalies are negative. The significance of composite anomalies is measured by comparing the magnitude of composite anomalies with the standard deviation (or inter-member spread) of individual anomalies with respect to the composite anomalies in the same group. In the following, we first discuss the cases when SEIO and ECP SSTs may act in concert for influencing SC rainfall, followed by the cases when only one of them plays the role for SC rainfall. The following description corresponds to the cases when SC rainfall is above normal, but it also applies to the cases when SC rainfall is below normal except for a switch in the sign of anomalies.

4.1 Combined influences of ECP and SEIO SSTs

Figure 7 shows composite anomalies of SST, 850 hPa winds, 200 hPa winds, and 500 hPa vertical velocity for cases when SEIO and ECP SSTs may act in concert. Left panels correspond to the cases when the SEIO SST anomalies are of the same signs as and the NINO4 SST anomalies are of the signs opposite to SC rainfall anomalies during 1951–1974, and rights panels to the cases when the SEIO SST anomalies are opposite to and the NINO4 SST anomalies are of the same signs as SC rainfall anomalies during 1975–2007.

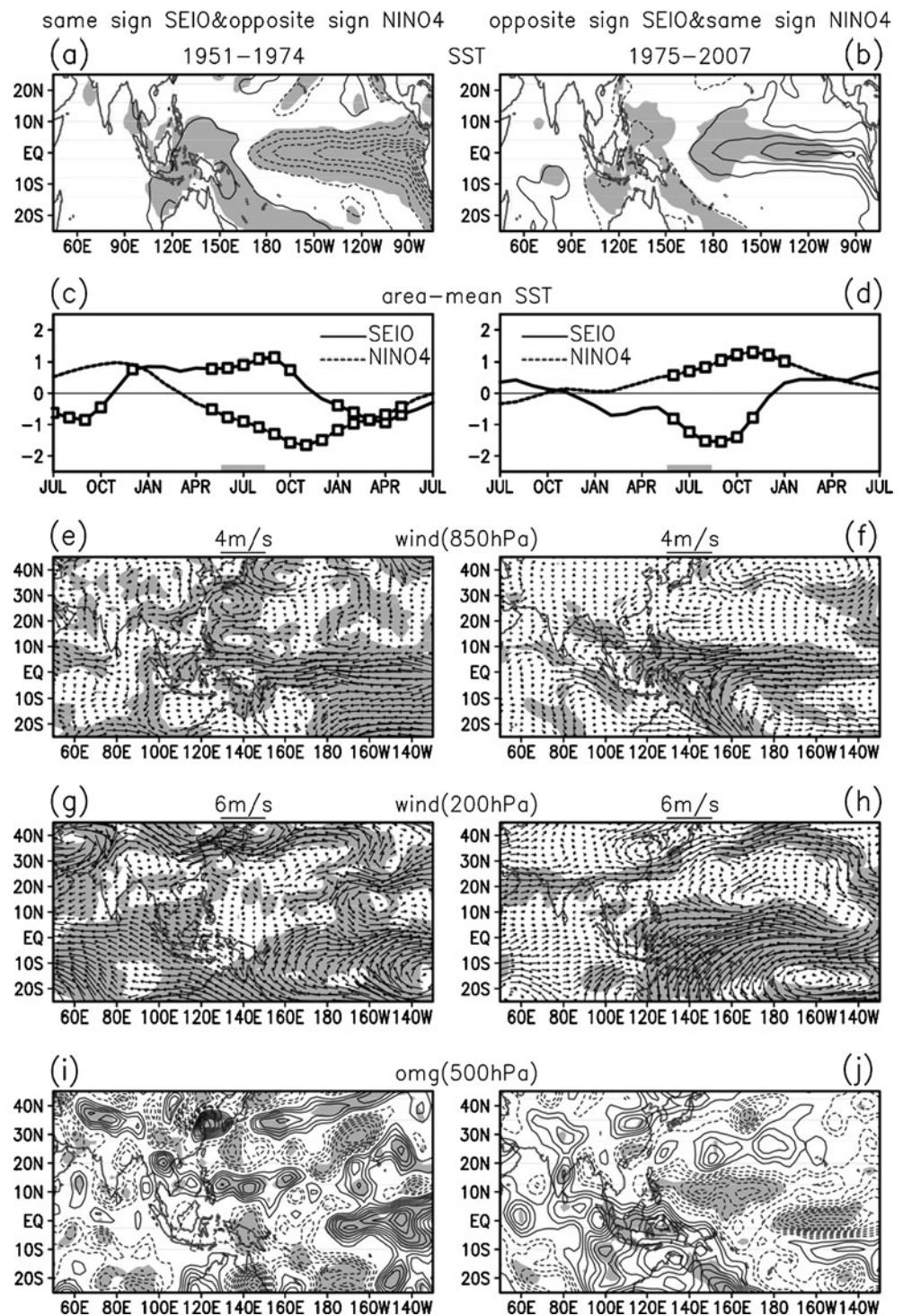
During 1951–1974, the SST anomalies show an obvious east–west contrast in the equatorial Pacific (Fig. 7a). Positive SST anomalies are seen in SEIO, but the center is near the northwest coast of Australia. The temporal evolution of NINO4 SST anomalies indicates a developing La Niña (Fig. 7c). Positive SEIO SST anomalies start to appear in preceding winter, following warm NINO4 SST anomalies, indicating an impact of ENSO on the Indian Ocean (Klein et al. 1999).

Table 2 Years when JJA SEIO or NINO4 SST anomalies have the sign same as or opposite to SC JJA rainfall during 1951–1974 and 1975–2007

	SEIO SST		NINO4 SST	
	1951–1974	1975–2007	1951–1974	1975–2007
Same sign	1951, 1955, 1956, 1964, 1965, 1967, 1968, 1971, 1973	1980, 1988, 2000, 2001, 2004, 2005	1956, 1966, 1967, 1971	1975, 1978, 1980, 1982, 1984, 1986, 1989, 1996, 1997, 1998, 2002, 2003, 2006
Opposite sign	1966	1975, 1976, 1978, 1979, 1982, 1984, 1986, 1989, 1992, 1994, 1996, 1997, 1998, 2006	1951, 1953, 1954, 1955, 1957, 1963, 1964, 1965	1988

Entries in bold denote years when one of the SST anomalies has the sign same as and the other has the sign opposite to SC rainfall anomalies. Entries in italics denote years when the NINO4 SST anomalies are opposite to SC rainfall anomalies and SEIO SST is normal during 1951–1974 or years when the SEIO SST anomalies are opposite to SC rainfall anomalies and NINO4 SST is normal during 1975–2007

Fig. 7 Composite anomalies of JJA SST (a, b), 3-monthly running mean SEIO (solid curve) and NINO4 (dashed curve) SST (c, d), JJA 850 hPa winds (e, f), JJA 200 hPa winds (g, h), and JJA 500 hPa p -vertical velocity (i, j) for the cases that the SEIO JJA SST anomalies are of the same sign as and the NINO4 JJA SST anomalies are of opposite sign to JJA SC rainfall anomalies during 1951–1974 (left) and for the cases that the SEIO JJA SST anomalies are of the opposite sign to and the NINO4 JJA SST anomalies are of the same sign as JJA SC rainfall during 1975–2007. In (a, b), the contour interval is 0.2°C and contours with the magnitude of less than 0.2°C are suppressed. In (i, j), the contour interval is 0.002 Pa s^{-1} and contours with the magnitude less than 0.002 Pa s^{-1} are suppressed. The wind scales are shown at the top of respective panels. Shading or marks denotes the magnitude of composite anomalies larger than the spread of anomalies



The wind anomalies over the tropical Pacific feature responses to anomalous cooling associated with negative SST anomalies in the central and eastern equatorial Pacific. Anomalous easterlies are observed at lower-level (Fig. 7e) and anomalous westerlies are observed at upper-level with two anomalous cyclones lying to the north and south of the equator (Fig. 7g). There is a wave train over the WNP and East Asia at both lower-level and

upper-level wind fields (Figs. 7e, g) as well as at 500-hPa vertical velocity field (Fig. 7i). Anomalous descent and ascent are observed over the eastern and western equatorial Pacific, respectively (Fig. 7i), forming an east–west contrast, which is consistent with the SST contrast. These features indicate an intensification of the Walker cell over the equatorial Pacific. The vertical velocity anomalies over SEIO are weak (Fig. 7i).

The above-circulation anomalies appear to suggest that ECP SST plays a more important role compared with SEIO SST. The impact of the ECP SST anomalies on SC rainfall appears to be indirect. It first induces anomalous ascent over the Maritime Continent via an anomalous Walker circulation, as shown in previous studies (e.g., Wang et al. 2003). The anomalous heating over the Maritime Continent induces anomalous descent over the SCS and WNP through modulating the Hadley cell. The anomalous convection around the Philippines then excites a wave pattern along East Asia, with lower-level convergence and ascent over SC, leading to above-normal SC rainfall.

During 1975–2007, an east–west contrast of SST anomalies is seen in the eastern Indian Ocean and the Pacific Ocean (Fig. 7b). The SST anomalies in the SEIO are larger and located closer to the equator compared to 1951–1974. The temporal evolution of the NINO4 SST anomalies indicates a developing El Niño (Fig. 7d). SEIO SST anomalies develop in summer. The 850 hPa anomalous winds feature a large anticyclone covering the regions of northern Australia, the Maritime Continent, and the Bay of Bengal, which is connected with westerlies over the equatorial western and central Pacific (Fig. 7f). Cyclonic winds dominate over SC and low-latitude WNP. The 200 hPa winds feature cross-equatorial northerlies over the Maritime Continent (Fig. 7h), opposite to those at 850 hPa. Two large anticyclones straddle over the tropical Pacific with easterlies over the equatorial western and central Pacific (Fig. 7h). The 500 hPa vertical motion displays descent over the SEIO and the Maritime Continent and ascent over the WNP and ECP (Fig. 7j). Over eastern China is a north–south dipole pattern.

The circulation anomalies indicate a concerted contribution of the ECP and SEIO SST anomalies. The tropical Pacific wind anomalies feature a response to anomalous warming in the ECP. Anomalous lower-level cyclone over the WNP may be interpreted as a Rossby wave type response to anomalous heating over the ECP. Negative SST anomalies in the SEIO induce lower-level cross-equatorial southerlies over the Maritime Continent, leading to lower-level divergence and descent over SEIO and the Maritime Continent. Upper-level cross-equatorial northerlies contribute to upper-level divergence, ascent, and lower-level cyclone over the WNP.

The SST anomalies in the SCS and WNP appear to be a response to the atmospheric changes. Negative SST anomalies correspond to anomalous low-level cyclone and anomalous ascent. Anomalous westerlies to the south of cyclone enhance monsoon westerlies and increase surface evaporation. Anomalous ascent leads to more clouds and suppresses downward shortwave radiation. These conditions favor the SST cooling.

4.2 Individual influences of ECP and SEIO SSTs

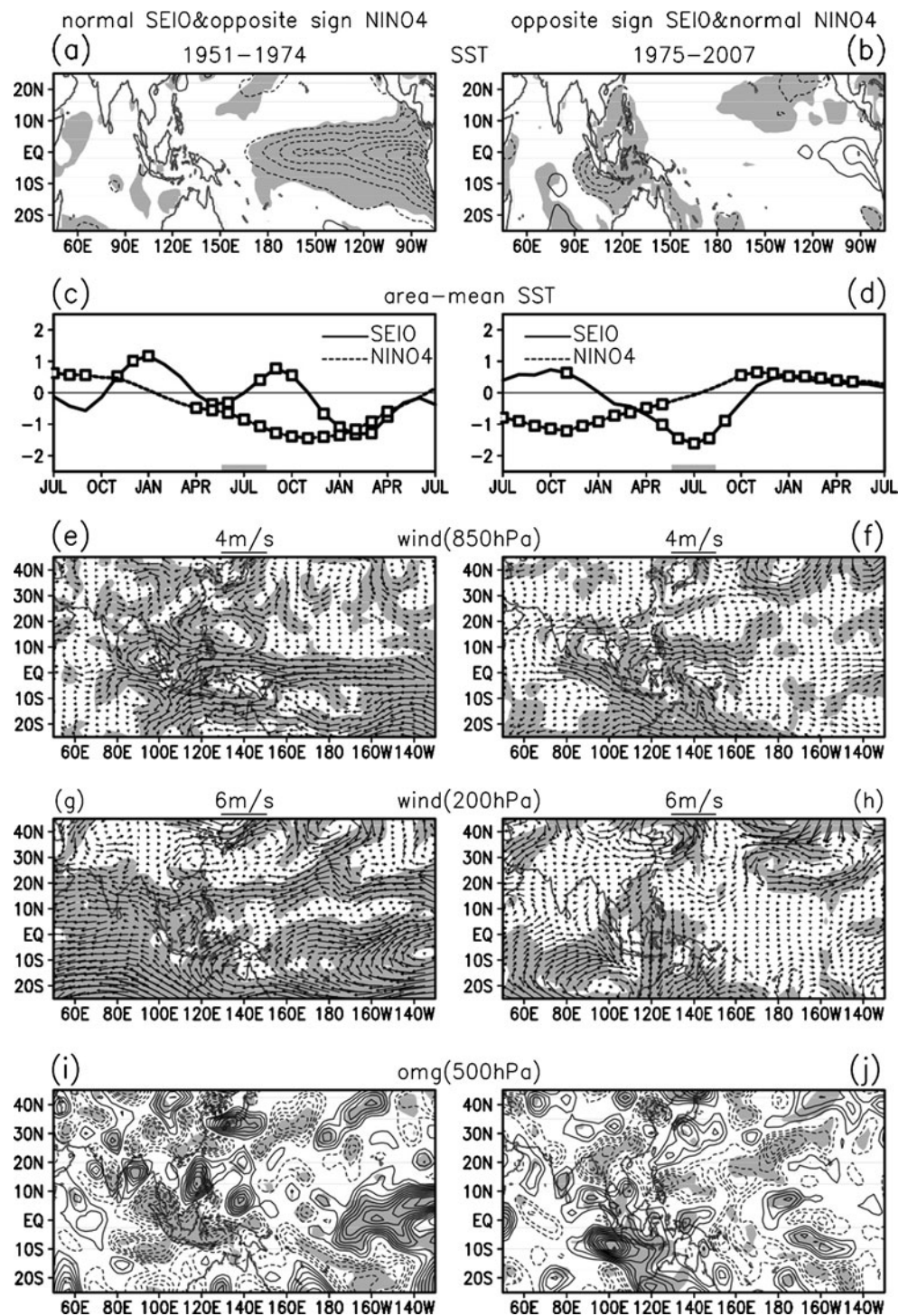
Figure 8 is similar to Fig. 7 except for the cases when either SEIO or ECP SST is near normal and thus only ECP or SEIO SST anomalies may play the role for SC rainfall variability. The left panels correspond to the cases when SEIO SST is near normal and thus only ECP SST forcing may contribute to SC rainfall during 1951–1974. The right panels correspond to the cases when NINO4 SST is near normal and thus only SEIO SST forcing may contribute to SC rainfall during 1975–2007.

During 1951–1974, negative SST anomalies are observed in the ECP and SST anomalies are weak in the SEIO (Fig. 8a). The temporal evolution of NINO4 SST anomalies indicates a developing La Niña (Fig. 8c). The wind and vertical velocity anomalies are similar to those in left panels of Fig. 7. For example, an anomalous anticyclone is present over the SCS and WNP and an anomalous cyclone over SC at 850 hPa (Fig. 8e). A meridional wave pattern extends from the WNP to the high latitudes of East Asia as seen in 850 hPa and 200 hPa winds and 500 hPa vertical velocity (Figs. 8e, g, i). At 500 hPa, there is ascent over SC (Fig. 8i). In comparison, lower-level convergence, rising motion, and upper-level divergence over the Maritime Continent are located more westward. Nevertheless, the impact of ECP SST forcing appears to be indirect, through the paths as described above corresponding to the cases in left panels of Fig. 7, i.e., though anomalous heating over the Maritime Continent via a Walker circulation, anomalous heating over the SCS and WNP via an Hadley cell, and a wave pattern along East Asia.

During 1975–2007, negative SST anomalies are observed in the SEIO (Fig. 8b), which are much larger compared with those in Fig. 7b. These are preceded by La Niña events in the preceding winter and El Niño events in the following winter (Fig. 8d). The 850 hPa wind and 500 hPa vertical velocity over the eastern Indian Ocean, the Maritime Continent, the SCS, the WNP, and SC as well as the 200 hPa winds over the eastern Indian Ocean and the Maritime Continent resemble those seen in the right panels of Fig. 7. For example, a large lower-level anticyclone overlies the regions surrounding the Maritime Continent and cyclonic winds are seen over the WNP and SC (Fig. 8f). Descent dominates the SEIO and ascent is over the WNP and SC (Fig. 8j). The upper-level winds over the Maritime Continent are northerly and convergence is seen over SEIO (Fig. 8h). These similarities illustrate the independent contribution of SEIO SST anomalies seen in the right panels of Fig. 7. The upper-level winds over middle-latitude East Asia show differences from Fig. 7h, which may be related to the lack of ECP SST forcing.

While the above analysis demonstrates that the SC summer rainfall variability can be induced independently by SST anomalies in SEIO and ECP, there are many more

Fig. 8 Same as Fig. 7 except for the cases that the SEIO JJA SST is normal and the NINO4 JJA SST anomalies are of opposite signs to JJA SC rainfall anomalies during 1951–1974 and the cases that the SEIO JJA SST anomalies are of the opposite signs to JJA SC rainfall anomalies and the NINO4 JJA SST is during 1975–2007



cases that the two SSTs contribute coherently (Table 2). In most of the years listed in Table 2, the SEIO and NINO4 SST anomalies are opposite to each other. There are only 4 years (1956, 1967, 1971, and 1980) in which the NINO4 and SEIO SST anomalies are of the same sign. Thus, in observations, the SEIO and NINO4 SST anomalies tend to act in concert with each other in influencing the SC summer rainfall variability.

Because of the co-variability of SST in the tropical Indo-Pacific regions, both SEIO and NINO4 SST anomalies appear to contribute to SC summer rainfall variability. To understand relative roles of the SST anomalies in the two regions, we have performed a partial correlation analysis for 1951–1971 and 1978–1998, respectively. The partial correlation coefficients between SC rainfall and SEIO SST after removing the impact of NINO4 SST are 0.41 and

−0.68 for 1951–1971 and 1978–1998, respectively. The partial correlation coefficients between SC rainfall and NINO4 SST anomalies after removing the impact of SEIO SST are −0.42 and −0.07 for 1951–1971 and 1978–1998, respectively. From these partial correlations, it appears that SEIO and NINO4 SST anomalies are equally important during 1951–1971, but SEIO SST anomalies play a much larger role than NINO4 SST anomalies during 1978–1998.

5 Discussions of reasons for interdecadal change in the rainfall–SST relationship

This section discusses the plausible causes for the observed interdecadal change in the rainfall–SST relationship. These discussions are based on previous relevant studies and the evidence seen in the regression and composite fields in this study. Some of the previous studies are not specifically about SC summer rainfall, but the reasons proposed for the interdecadal change in the relationship are relevant and thus are included in the discussions. Note that the specific periods used in contrasting the relationship in this study are not exactly the same as those in previous studies.

One factor that may have contributed to the interdecadal change in the rainfall–SST relationship is the mean state change, in particular, the change in the WNP subtropical high (Chang et al. 2000; Wu and Wang 2002; Ding et al. 2010). The WNP subtropical high experienced an intensification and expanse in the late 1970s in association with the increase of mean SST in the tropical Indo-Pacific Ocean (Hu 1997; Chang et al. 2000; Wu and Wang 2002; Mao et al. 2010). This change in mean WNP subtropical high influences the location of anomalous anticyclone over the WNP and thus the location of rainfall anomalies induced by SST anomalies. Chang et al. (2000) indicated that during 1951–1977, May–June rainfall in the southeast coastal area of China and the Yangtze River valley displayed an in-phase interannual variation because the anomalous WNP anticyclone is slightly farther away from the southeast coast of China, whereas during 1978–1996 the anomalous anticyclone is more northward, leading to out-of-phase interannual variations of May–June rainfall in the southeast coast and Yangtze River valley of China. As such, an interdecadal change is observed in the relationship between southeast China May–June rainfall and tropical Pacific SST around the late-1970s. Ding et al. (2010) also considered the interdecadal change in the WNP subtropical high as a plausible cause for the change in the relationship between the Indian Ocean SST and the East Asian summer monsoon.

The change in the location of the mean WNP subtropical high is related to the change in the location of mean convection, which affects the location of anomalous

convective heating over the WNP and the atmospheric response (Wu and Wang 2002). This sensitivity of anomalous convection and circulation response to the mean state has been demonstrated by numerical experiments of an atmospheric general circulation model (AGCM). The anomalous low-level anticyclone and convection over the WNP, in response to the same ENSO-type SST forcing, extends to higher latitude under a higher mean SST, which leads to a shift in the wave pattern along East Asia and contributes to the change in the North China summer rainfall-ENSO relationship around the late 1970s (Wu and Wang 2002).

During 1951–1971, the mean WNP subtropical high and convection are located at lower latitudes (Chang et al. 2000; Wu and Wang 2002). As such, anomalous descent and lower-level anticyclone induced by positive SEIO SST anomalies sit at lower latitudes, i.e., in the SCS (Fig. 4a). Correspondingly, an anomalous vertical circulation lies between SEIO and SCS (Fig. 6a). The suppressed convection over the SCS in turn induces another anomalous vertical circulation with anomalous ascent over SC, enhancing SC summer rainfall. Thus, positive SEIO SST anomalies are accompanied by above-normal SC summer rainfall. During 1978–1998, because of the expansion of the WNP subtropical high and enhanced mean convection, anomalous ascent and lower-level cyclone induced by negative SEIO SST anomalies reach higher latitudes, i.e., over SC (Fig. 4b). An anomalous vertical circulation directly connects SEIO and SC (Fig. 6b). Thus, negative SEIO SST anomalies correspond to below-normal SC summer rainfall.

Another factor discussed by Ding et al. (2010) is the weakened mean land–sea thermal gradient accompanying the warming of the tropical Indo-Pacific Oceans and the cooling of the Asian land. They argued that the summer SST anomalies superposed on a higher mean SST in 1978–2000 contributed to a stronger influence of the land–sea thermal contrast in weakening the East Asian summer monsoon. Further work is needed to illustrate which part of the mean change (the subtropical high or the land–sea thermal contrast) is more important in modulating the response of the atmospheric circulation to anomalous SST forcing.

Ding et al. (2010) proposed that the influence of the summer IOD on the East Asian summer monsoon may be related to the relationship of the IOD to ENSO in preceding winter. During 1953–1975, the summer IOD events exert an independent influence on the East Asian summer monsoon under the weak La Niña pattern in the eastern equatorial Pacific. During 1978–2000, the influence of the summer IOD events on the East Asian summer monsoon is disrupted by the opposite influence of El Niño events of the previous winter so that the relationship between the

summer IOD and the East Asian summer monsoon is weakened. The present study indicates that the preceding SST anomalies in the eastern equatorial Pacific are not related to summer SC rainfall both before and after the mid-1970s (Figs. 1a–b). This difference appears because the East Asian summer monsoon index defined by Li and Zeng (2002) mainly represents the variability of summer rainfall in the middle and lower reaches of the Yangtze River valley (Ding et al. 2010).

Another plausible reason for the change in the SC summer rainfall–SST relationship may be the location and magnitude of SST anomalies in the SEIO. The SEIO SST anomalies are larger and located more northwestward after the mid-1970s than before the mid-1970s (Figs. 7a–b and 1b–c). This indicates a larger SST forcing after the mid-1970s than before the mid-1970s, which is supported by differences in anomalies of vertical motion (Figs. 4e–f and 7i–j), lower-level winds over SEIO and the Maritime Continent (Figs. 4a–b and 7e–f), and upper-level divergence/convergence over SEIO (Fig. 5a–b). The larger SEIO SST forcing after the mid-1970s leads to an expanse of circulation response to higher latitudes north of the equator compared to that before the mid-1970s.

Further studies are needed to understand the causes for the interdecadal change in the rainfall–SST relationship and to illustrate the relative contribution of different factors for the change. One way would be to perform numerical experiments with AGCMs with different mean and anomalous SST forcing specified. We have conducted such experiments with two AGCMs with SST anomalies specified in the SEIO region. Unfortunately, the models have difficulty in producing reasonable circulation and rainfall anomalies over the Maritime Continent, likely because of the complexity of the topography and the model deficiency in this critical region.

6 Summary and discussions

The present study reveals an obvious interdecadal change in the relationship between SC summer rainfall and tropical Indo-Pacific SST around early to mid-1970s. During the 1950s and 1960s, above-normal SC summer rainfall is associated with positive SST anomalies in the SEIO and negative SST anomalies in the ECP. During the 1980s and 1990s, in contrast, above-normal SC summer rainfall follows colder SST in the SEIO and warmer SST in the ECP.

Consistent with the change in the rainfall–SST correlation, there are more cases of same-sign relationship than opposite-sign relationship between the SEIO SST and SC rainfall anomalies before the mid-1970s, but there are more cases of opposite-sign relationship than same-sign relationship after the mid-1970s. On the contrary, there are more

cases of opposite-sign relationship than same-sign relationship between the NINO4 SST and SC rainfall before the mid-1970s, but there are more cases of same-sign relationship than opposite-sign relationship after the mid-1970s.

The present study identifies different features in the atmospheric circulation anomalies associated with SC summer rainfall between the two periods. During the 1950s and 1960s, there are two meridional cells between SEIO and SC: one between SEIO and northern SCS and the other between northern SCS and SC. The connection between SEIO and SC is indirectly through a common branch over northern SCS. During the 1980s and 1990s, a single meridional cell links directly SEIO and SC. As such, anomalous heating induced by positive SST anomalies in SEIO is accompanied by anomalous ascent and above-normal rainfall over SC in the former period, but leads to anomalous descent and below-normal rainfall over SC in the latter period.

Composite analysis shows that SEIO and NINO4 SST anomalies act in concert in many years, affecting the atmospheric circulation and rainfall over southern China. They can also contribute to SC summer rainfall variability independently. In comparison, there are more cases that the contributions of both SST anomalies are in concert because of the co-variability between the Indian and Pacific SSTs.

The change in the relationship between SC summer rainfall and tropical Indo-Pacific SSTs may be attributed to two factors. One is the sensitivity of atmospheric response to the change in the mean state, as discussed in previous studies (Chang et al. 2000; Wu and Wang 2002). The stronger and larger mean WNP subtropical high in the recent decades leads to a shift of the atmospheric response to tropical SST forcing to higher latitudes. As such, SEIO SST anomalies may directly lead to circulation and rainfall changes over SC. The other is the change in SEIO SST anomalies that are much larger and located closer to the equator. The larger SST forcing induces atmospheric circulation change that influences SC climate more directly.

There are two typical rainy seasons over SC: one occurs in early summer (May to mid-June) and the other in late summer (mid-July to August). The rainfall in early summer is mainly related to summer monsoon activity, while the rainfall in late summer is partly contributed by tropical cyclones. One question is whether the interdecadal change in the SST–rainfall relationship exists for both rainy seasons or only in one of them. To address this question, we have examined the SST–rainfall relationship for May–June and July–August separately. Results indicate that the interdecadal change in the SST–rainfall relationship is weak for May–June, but an obvious change is observed for July–August.

Summer monsoon rainfall over Asia exhibits decadal variability with alternative above-normal and below-normal

rainfall epochs (e.g., Kripalani and Kulkarni 1997a, b, 2001). Previous studies have indicated that the impact of ENSO is modulated by the decadal variability in monsoon rainfall. For example, the impact of El Niño (La Niña) events on the Indian summer rainfall is more severe during the below-normal (above-normal) rainfall epochs (Kripalani and Kulkarni 1997a). Whether this interdecadal modulation of El Niño and La Niña impacts exists for SC summer rainfall needs to be examined with longer rainfall data.

Acknowledgments The authors thank three anonymous reviewers for their comments. RW acknowledge the support of a Direct Grant from the Chinese University of Hong Kong (2021090). HG and KH are supported by National Natural Science Foundation of China (grants 40890155, U0733002, and 40810059005).

References

- Annamalai H, Xie S-P, McCreary JP, Murtugudde R (2005) Impact of Indian Ocean sea surface temperature on developing El Niño. *J Climate* 18:302–319
- Chang C-P, Zhang Y-S, Li T (2000) Interannual and interdecadal variations of the East Asian summer monsoon and tropical Pacific SSTs. Part II: Meridional structure of the monsoon. *J Climate* 13:4326–4340
- Chen L-T, Wu R (2000) Interannual and decadal variations of snow cover over Qinghai-Xizang Plateau and their relationships to summer monsoon rainfall in China. *Adv Atmos Sci* 17:18–30
- Chen M, Xie P, Janowiak JE, Arkin PA (2002) Global land precipitation: A 50-yr monthly analysis based on gauge observations. *J Hydrometeorol* 3:249–266
- Ding R-Q, Ha K-J, Li J-P (2010) Interdecadal shift in the relationship between the East Asian summer monsoon and the tropical Indian Ocean. *Clim Dyn* 34:1059–1071. doi:10.1007/s00382-009-0555-2
- Hu Z-Z (1997) Interdecadal variability of summer climate over East Asia and its association with 500 hPa height and global sea surface temperature. *J Geophys Res* 102:19403–19412
- Huang B, Kinter JL III (2002) Interannual variability in the tropical Indian Ocean. *J Geophys Res* 103:3199. doi:10.1029/2001JC001278
- Huang R-H, Sun F-Y (1992) Impacts of the tropical western Pacific on the East Asian summer monsoon. *J Meteor Soc Japan* 70:243–256
- Huang R-H, Wu Y-F (1989) The influence of ENSO on the summer climate change in China and its mechanism. *Adv Atmos Sci* 6:21–32
- Huang R-H, Zhou L-T, Chen W (2003) The progress of recent studies on the variabilities of the East Asian monsoon and their causes. *Adv Atmos Sci* 20:55–69
- Inoue T, Matsumoto J (2004) A comparison of summer sea level pressure over East Eurasia between NCEP-NCAR reanalysis and ERA-40 for the period 1960–99. *J Meteor Soc Japan* 82:951–958
- Kalnay E et al (1996) NCEP/NCAR 40-year reanalysis project. *Bull Amer Meteor Soc* 77:437–471
- Klein SA, Soden BJ, Lau N-C (1999) Remote sea surface temperature variations during ENSO: evidence for a tropical atmospheric bridge. *J Climate* 12:917–932
- Kripalani RH, Kulkarni A (1997a) Climatic impact of El Niño/La Niña on the Indian Monsoon: a new perspective. *Weather* 52:39–46
- Kripalani RH, Kulkarni A (1997b) Rainfall variability over Southeast Asia-connections with Indian Monsoon and ENSO extremes: new perspectives. *Int J Climatol* 17:1155–1168
- Kripalani RH, Kulkarni A (2001) Monsoon rainfall variations and tele-connections over South and East Asia. *Int J Climatol* 21:603–616
- Lau K-M, Weng H-Y (2001) Coherent modes of global SST and summer rainfall over China: an assessment of the regional impacts of the 1997–98 El Niño. *J Climate* 14:1294–1308
- Li J-P, Zeng Q-C (2002) A unified monsoon index. *Geophys Res Lett* 29:1274. doi:10.1029/2001GL013874
- Lindzen RS, Nigam N (1987) On the role of sea surface temperature gradients in forcing low-level winds and convergence in the tropics. *J Atmos Sci* 44:2418–2436
- Mao J-Y, Chan JCL, Wu G-X (2010) Interannual variations of early summer monsoon rainfall over South China under different PDO background. *Int J Climatol*. doi:10.1002/joc.2129
- Saji NH, Goswami BN, Vinayachandran PN, Yamagata T (1999) A dipole mode in the tropical Indian Ocean. *Nature* 401:360–363
- Smith TM, Reynolds RW, Peterson TC, Lawrimore J (2008) Improvements to NOAA's historical merged land-ocean surface temperature analysis (1880–2006). *J Climate* 21:2283–2296
- Wang B, Wu R, Li T (2003) Atmosphere-warm ocean interaction and its impacts on Asian-Australian monsoon variation. *J Climate* 16:1195–1121
- Weng H-Y, Lau K-M, Xue Y (1999) Multi-scale summer rainfall variability over China and its long-term link to global sea surface temperature variability. *J Meteor Soc Japan* 77:845–857
- Weng H, Wu G-X, Liu Y-M, Behera SK, Yamagata T (2009) Anomalous summer climate in China influenced by the tropical Indo-Pacific Oceans. *Clim Dyn*. doi:10.1007/s00382-009-0658-9
- Wu R, Kirtman BP (2007) Observed relationship of spring and summer East Asian rainfall with winter and spring Eurasian snow. *J Climate* 20:1285–1304
- Wu T-W, Qian Z-A (2003) The relation between the Tibetan winter snow and the Asian summer monsoon and rainfall: an observational investigation. *J Climate* 16:2038–2051
- Wu R, Wang B (2002) A contrast of the East Asian summer monsoon-ENSO relationship between 1962–77 and 1978–93. *J Climate* 15:3266–3279
- Wu R, Yeh S-W (2010) A further study of the tropical Indian Ocean asymmetric mode in boreal spring. *J Geophys Res* 115:D08101. doi:10.1029/2009JD012999
- Wu R, Hu Z-Z, Kirtman BP (2003) Evolution of ENSO-related rainfall anomalies in East Asia. *J Climate* 16:3742–3758
- Wu R, Kinter JL III, Kirtman BP (2005) Discrepancy of interdecadal changes in the Asian region among the NCEP-NCAR reanalysis, objective analyses, and observations. *J Climate* 18:3048–3067
- Wu R, Kirtman BP, Krishnamurthy V (2008) An asymmetric mode of tropical Indian Ocean rainfall variability in boreal spring. *J Geophys Res* 113:D05104. doi:10.1029/2007JD009316
- Xiao Z-N, Yan H-M, Li C-Y (2002) Relationship between dipole oscillation of SSTA of Indian Ocean region and precipitation and temperature in China. *J Trop Meteor* 8:121–131
- Xie P, Arkin PA (1997) Global precipitation: a 17-year monthly analysis based on gauge observations, satellite estimates, and numerical model outputs. *Bull Amer Meteor Soc* 78:2539–2558
- Xie S-P, Annamalai H, Schott FA, McCreary JP (2002) Structure and mechanisms of South Indian Ocean climate variability. *J Climate* 15:864–878
- Yang S, Lau K-M (1998) Influences of sea surface temperature and ground wetness on Asian summer monsoon. *J Climate* 11:3230–3246
- Yang S, Lau K-M (2006) Interannual variability of the Asian monsoon. In: Wang B (ed) *the Asian monsoon*. Springer, New York, pp 259–293
- Yang S, Xu L (1994) Linkage between Eurasian winter snow cover and regional Chinese summer rainfall. *Int J Climatol* 14:739–750

- Yang S, Lau K-M, Kim K-M (2002) Variations of the East Asian jet stream and Asian-Pacific-American winter climate anomalies. *J Climate* 15:306–325
- Zhang R-H, Sumi A, Kimoto M (1996) Impact of El Niño on the East Asian monsoon: a diagnostic study of the 86/87 and 91/92 events. *J Meteor Soc Japan* 74:49–62
- Zhang R-H, Sumi A, Kimoto M (1999) A diagnostic study of the impact of El Niño on the precipitation in China. *Adv Atmos Sci* 16:229–241
- Zhao P, Zhou Z-J, Liu J-P (2007) Variability of Tibetan spring snow and its associations with the hemispheric extratropical circulation and East Asian summer monsoon rainfall: an observational investigation. *J Climate* 20:3942–3955
- Zhu Y-M, Yang X-Q, Chen X-Y, Zhao S-S, Sun X-G (2007) Interdecadal variation of the relationship between ENSO and summer interannual climate variability in China. *J Trop Meteorol* 13(2):132–136